

Thin film channel waveguides fabricated in metalorganic chemical vapor deposition grown BaTiO₃ on MgO

D. M. Gill^{a)}

Department of Electrical and Computer Engineering, Northwestern University, Evanston, Illinois 60208

B. A. Block

Department of Materials Science and Engineering, Materials Research Center, Northwestern University, Evanston, Illinois 60208

C. W. Conrad

Department of Electrical and Computer Engineering, Northwestern University, Evanston, Illinois 60208

B. W. Wessels

Department of Electrical and Computer Engineering and Department of Materials Science and Engineering, Northwestern University, Evanston, Illinois 60208

S. T. Ho

Department of Electrical and Computer Engineering, Northwestern University, Evanston, Illinois 60208

(Received 10 July 1996; accepted for publication 4 September 1996)

We report on the fabrication of channel waveguides in epitaxial grown BaTiO₃ layers on MgO. Layers were prepared by metalorganic chemical vapor deposition. Ridge waveguides with ridge heights ranging from 15 to 200 nm were fabricated in a 0.2- μm -thick film. Single mode waveguide throughput, scattering loss, and mode profiles are reported. Coating waveguides with spin on glass significantly increase waveguide throughput. Throughputs of up to 10.4% were measured in 15 nm ridge waveguides which were 2.85 mm long and coated with spin on glass. Waveguide throughput is found to increase significantly with an increase in wavelength from 1.06 to 1.55 μm . © 1996 American Institute of Physics. [S0003-6951(96)03446-8]

There is considerable interest in developing ferroelectric thin films for integrated optics. Applications include second-harmonic generation, high speed modulators, and gain devices. Thin film devices offer unique physical characteristics potentially superior to diffused waveguides fabricated in bulk ferroelectrics. For example, large index changes between the film and substrate enable highly confining waveguides to be formed.¹ The high confinement in thin film waveguides creates the potential for fast, low voltage electro-optic switching, facilitated by the small electrode separation allowed due to the small dimensions of these waveguides.² In addition, extremely high power densities are achievable with modest total powers, characteristics conducive to second-harmonic generation and low-threshold gain devices. A thin film geometry also enables large effective index changes to be made along the length of the waveguide with minimal difficulty. This makes these systems particularly attractive for applications involving integrated Bragg reflectors or photonic band gap geometries. A major challenge in the application of thin film waveguide systems is the fabrication of low loss channel waveguides.

BaTiO₃ is a potential thin film integrated optic host which exhibits an electro-optic effect much larger than that found in LiNbO₃.³ Furthermore, epitaxially grown BaTiO₃ doped with rare-earth ions, such as erbium, has potential as an active optical gain medium. The solid solubility of Er³⁺ ions in BaTiO₃ ($\sim 10^{21}/\text{cm}$) is about an order of magnitude higher than in LiNbO₃ ($\sim 10^{20}/\text{cm}$).⁴⁻⁶ In addition, for Er:LiNbO₃ amplifiers and lasers the Er³⁺ is thermally diffused

into an undoped bulk crystal resulting in high Er³⁺ concentrations very close to the surface of the waveguide^{4,7} while the optical mode profiles tend to peak below the surface.^{8,9} As a result, the overlap between the gain ion doping and light profiles is poor. Since Er:BaTiO₃ can be epitaxially grown¹⁰ (with an index change of $\Delta n \sim 0.7$ between the substrate and the film) the overlap between the dopant and light profiles will be far greater. These qualities should greatly reduce the size of potential integrated gain devices.

While there are numerous advantages to thin film ferroelectric waveguides, their application has been limited because of the difficulty in preparing materials with low optical losses. For a single mode waveguide, the film thickness must be between 150 and 600 nm. For films of this thickness, the optical field intensity at the surfaces and the interfaces can be quite high; consequently large optical losses result from surface scattering. In general, ferroelectric films tend to have a rms roughness of 10 nm or greater due to the three-dimensional island growth encountered in many systems. However, recently there have been improvements in deposition techniques resulting in films with roughness as low as 2 nm.¹¹ In this letter, we report on ridge waveguides in epitaxial BaTiO₃ prepared by metalorganic chemical vapor (MOCVD) deposition. Single mode waveguides with losses as low as 4 ± 2 dB/cm were fabricated.

Films were synthesized in a low pressure MOCVD reactor that has been previously described.¹² The metalorganic precursors employed were titanium tetra-isopropoxide and barium hexafluoroacetylacetonate⁹ tetraglyme. Argon was used as the carrier gas and O₂ bubbled through de-ionized water was used as the reactant gas. The introduction of water

^{a)}Electronic mail: gill@ece.nwu.edu

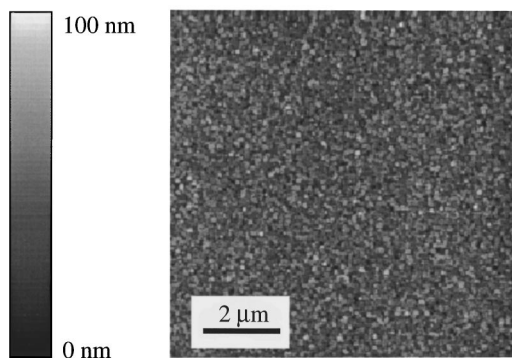


FIG. 1. Atomic force microscopy image of the surface of a 0.4- μm -thick BaTiO_3 film grown on a (001) oriented MgO crystal. The rms surface roughness is 7 nm.

vapor was necessary for removal of the fluorine as HF which results from the fluorinated barium precursor. The films were deposited on (001) oriented MgO crystals at 725 $^\circ\text{C}$ with a growth rate of approximately 100 nm/h. The films are transparent and appear specular to the unaided eye. X-ray diffraction indicated that the films were phase pure and had their crystallographic a -axis (100) aligned normal to the plane of the film. Epitaxial alignment of the film to the substrate was confirmed with phi scans of the off-axis {220} planes in the BaTiO_3 crystal lattice and the requisite fourfold symmetry was observed. It is assumed that the [010] and the [001] directions are randomly aligned to the [100] and [010] directions of the MgO substrate. Atomic force microscopy was used to analyze the surface morphology of the films. Figure 1 shows the morphology of a 0.3- μm -thick BaTiO_3 film on MgO with a rms surface roughness of 7 nm. The roughness is mainly due to columnar subgrains. The rms roughness is weakly dependent on thickness, as shown in Fig. 2.

Waveguides were fabricated in a 0.2- μm -thick BaTiO_3 film, with a rms surface roughness of 9 nm, using a 1% HF in water etch. Waveguides with ridge heights ranging from 15 to 200 nm and widths ranging from 2 to 6 μm were fabricated. Etching times ranged from 30 to 50 s. The 15 and 200 nm waveguides were coated with about 0.5 μm of spin on glass (SOG-Allied Signal 311). The processed guides were cleaved and light was end fired into the waveguides

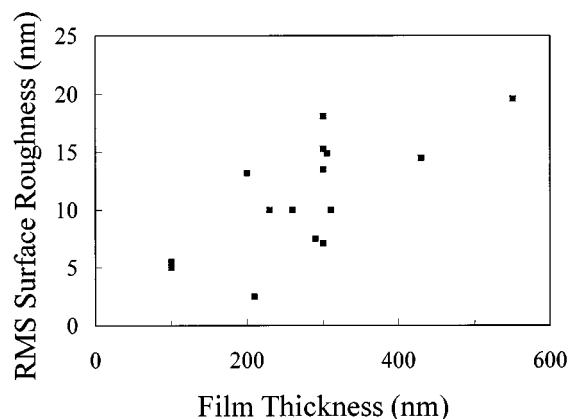


FIG. 2. Surface roughness vs film thickness for various BaTiO_3 films grown on MgO .

TABLE I. Throughput and scattering loss measurements from the three samples investigated. The scattering losses stated represent the average of the forward and reverse propagating measurements. The margin of error indicates the difference between the forward and reverse measurements. Variations in the scattering loss measured for forward and reverse propagation indicates the scattering loss is changing along the length of the waveguide.

Sample number	Ridge height (nm)	SiO_2 coating	Throughput (percent)	Scattering loss (dB/cm)
1	15	Yes	10.4	5 ± 5
2	200	Yes	6.8	8 ± 2
3	35	No	4.1	18 ± 4

(coupled with lenses). Waveguide loss, mode output profiles, and total throughput were measured with $\lambda = 1.55 \mu\text{m}$ light. The total throughput was also measured at $\lambda = 1.3$ and 1.06 μm in the highest throughput waveguide. Scattering loss measurements were made by focusing an enlarged image of the waveguide on a vidicon camera with a microscope objective lens and measuring the reduction in scattered light along the length of the waveguide. Care was taken to ensure that the response of the vidicon camera was linear in the measurement region. This loss measurement technique is valid provided the scattering is uniform along the length of the waveguide. Waveguides fabricated with thickness, roughness, or compositional variations will also show corresponding changes in scattering efficiency along their length, which can give erroneous scattering loss measurements. Consequently, the measured scattering loss can change when the sample is remeasured with the light propagating in the opposite direction. However, the throughput of such waveguides will remain the same regardless of the direction of light propagation. Therefore, throughput measurements are used to determine which sample shows the lowest loss and the scattering loss measurements, in conjunction with the throughput results, are used to estimate the input coupling efficiency. The throughput measurements are made by comparing the intensity of light which passes through the coupling lenses with and without the sample in place. The mode is apertured before the detector so as to avoid the inclusion of substrate modes in the measured output.

Table I shows the throughput and scattering loss measurements for coupled 1.55 μm light in the three pieces. The samples are listed in ascending order in terms of their loss, sample 1 having the lowest loss and sample 3 having the highest loss (as shown by their throughput measurements). The two samples coated with SOG show the highest throughput. This is most likely caused by a reduction in scattering from the guide's surface and sidewalls due to a decrease in index difference between the scattering centers and the waveguide surroundings. Figures 3(a)–3(c) show that the 1.55 μm light profiles from 6- μm -wide waveguides are all single mode on samples 1–3, respectively. The accuracy of the measured mode width is limited by the resolving power of the output coupling lens (limit of resolution $\sim 1.7 \mu\text{m}$). The vertical mode profiles for the SOG and non-SOG coated waveguides are both calculated to have a 0.3 μm full width at half-maximum. Therefore, the large increase in throughput with SOG coating is predominantly due to a reduction in

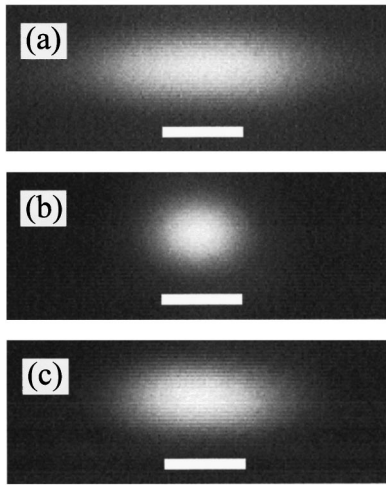


FIG. 3. Measured mode output profiles of $1.55 \mu\text{m}$ light coupled out of (a) a 15 nm ridge waveguide coated with spin on glass; (b) a fully etched (200 nm) ridge sample coated with spin on glass; (c) a 35 nm ridge waveguide with no spin on glass coating. Waveguides were patterned to be $6 \mu\text{m}$ wide, however, variations in waveguide widths are expected due to undercutting during the etching process. The scaling bar at the bottom of each picture represents a $3 \mu\text{m}$ length.

sidewall and surface scattering, as opposed to a change in coupling efficiency. Comparing samples 1 and 2 indicates that the lightly etched waveguides also show a higher throughput. Sample 1 (15 nm ridges/SOG coated) shows a maximum throughput of 10.4% measured in a $5 \mu\text{m} \times 2.85 \text{ mm}$ waveguide. Sample 2 (fully etched to the substrate, $0.2 \mu\text{m}$) shows an intermediate throughput of 6.8% for a $6 \mu\text{m} \times 2.35 \text{ mm}$ waveguide. The lowest throughput was shown by sample 3 (35 nm ridges/no SOG coating) which had a throughput of 4.1% in a $6 \mu\text{m} \times 2.40 \text{ mm}$ waveguide. Table I also shows the results from scattering loss measurements taken on the three samples. These results are presented with an error margin since we measured different scattering losses in the waveguides when the light was coupled into the pieces from different directions. It should be noted that we measured identical throughputs on our waveguides regardless of the direction of light propagation in the samples. The differences in scattering loss measurements are most likely caused by variations in the thickness of our film. This indicates that the propagation losses have not been minimized and further improvements in total throughput are expected. Sample 2, however, shows similar scattering loss measurements for both propagation directions in the waveguide. We therefore used the scattering loss and throughput measurements from this waveguide to estimate the input coupling efficiency. Assuming the loss in sample 2 is $\sim 10 \text{ dB/cm}$ we get an input coupling efficiency of $\sim 14\%$. In this calculation we assume a 17% reflection at the output of the waveguide due to the light passing from the BaTiO_3 ($n \sim 2.4$) to the air. If we also assume a 14% input coupling efficiency for samples 1 and 3 then the calculated loss for these two samples is ~ 2 and $\sim 19 \text{ dB/cm}$, respectively. Assuming a 17.5% input coupling efficiency the scattering losses are calculated to be ~ 5 , 14 , and 23 dB/cm for samples 1–3, respectively.

Table II shows the throughput versus wavelength measurements. The throughput is shown to be strongly dependent on wavelength. The large increase in throughput from

TABLE II. Throughput measurements from sample 1 for various wavelengths of light.

Wavelength (μm)	Throughput (percent)
1.55	10.4
1.3	6.6
1.06	0.1

1.06 to $1.55 \mu\text{m}$ is no doubt caused, in part, by a reduction in Rayleigh scattering efficiency with an increase in wavelength. The Rayleigh scattering efficiency may also be decreased by a reduction in birefringence ($\sim 10\%$) at the longer wavelengths, resulting in at longer wavelengths smaller index fluctuations due to subgrain misorientation.¹³

In conclusion, single mode ridge waveguides were fabricated using an epitaxial BaTiO_3 thin film prepared by MOCVD. Waveguides with losses of $\sim 4 \pm 2 \text{ dB/cm}$ were fabricated. Propagation losses and lateral mode confinement were found to be lower in lightly etched ridge samples. An approximate twofold increase in throughput was seen in waveguides coated with SOG. Loss also decreased dramatically with an increase in the wavelength ($\lambda = 1$ to $1.55 \mu\text{m}$) of the propagating light. We expect that propagation losses can be further reduced by growing films of the proper thickness and improving thickness uniformity.

The authors would like to thank D. Studebaker and Professor T. J. Marks for providing the $\text{Ba}(\text{hfa})_2$ tetraglyme precursor used in film growth. This work is supported by AFOSR/ARPA under Award No. F49620-96-1-0262 and the MRL Program of the National Science Foundation at the Materials Research Center of Northwestern University under Award No. DMR-9120521. This work made extensive use of the MRL central facilities.

¹F. J. Walker, R. A. McKee, Huan-wun Yen, and D. E. Zelmon, *Appl. Phys. Lett.* **65**, 1495 (1994).

²D. K. Fork, F. Armani-Leplingard, and J. J. Kingston, *Materials Research Society Symposium 12*, Ferroelectric Thin Films IV, Boston, MA, 29 November–2 December 1994 (unpublished).

³R. C. Alferness, *IEEE Trans. Microwave Theory Tech.* **MTT-30**, 1121 (1982).

⁴Ch. Buchal and S. Mohr, *J. Mater. Res.* **6**, 134 (1991).

⁵B. A. Block and B. W. Wessels, *Mater. Res. Soc. Symp. Proc.* **415**, 175 (1996).

⁶C. Eylem, G. Saghi-Szabo, B. H. Chen, B. Eichhorn, J. L. Peng, R. Greene, L. Salamanca-Riba, and S. Nam, *Chem. Mater.* **4**, 1038 (1992).

⁷D. M. Gill, A. Judy, L. McCaughan, and J. C. Wright, *Appl. Phys. Lett.* **60**, 1067 (1992).

⁸C. H. Huang, L. McCaughan, and D. M. Gill, *J. Lightwave Technol.* **12**, 803 (1994).

⁹M. Dinand and W. Sohler, *IEEE J. Quantum Electron.* **30**, 1267 (1994).

¹⁰B. A. Block and B. W. Wessels, *Integr. Ferroelectr.* **7**, 25 (1995).

¹¹M. J. Nystrom, B. W. Wessels, W. P. Lin, G. K. Wong, D. A. Neumayer, and T. J. Marks, *Appl. Phys. Lett.* **66**, 1726 (1995).

¹²L. A. Wills, W. A. Feil, B. W. Wessels, L. M. Tonge, and T. J. Marks, *J. Cryst. Growth* **107**, 712 (1991).

¹³A. R. Johnston, *J. Appl. Phys.* **42**, 398 (1971).